

Threshold voltage shift and formation of charge traps induced by light irradiation during the fabrication of organic light-emitting diodes

Yutaka Noguchi¹, Naoki Sato, Yuya Tanaka, Yasuo Nakayama, and Hisao Ishii

Citation: *Appl. Phys. Lett.* **92**, 203306 (2008); doi: 10.1063/1.2936084

View online: <http://dx.doi.org/10.1063/1.2936084>

View Table of Contents: <http://aip.scitation.org/toc/apl/92/20>

Published by the [American Institute of Physics](#)

A close-up photograph of a single metal needle protruding from a large, textured haystack of dry straw. The background is a soft-focus field of golden-brown grass or hay under a bright sky.

**FIND THE NEEDLE IN THE
HIRING HAYSTACK**

POST JOBS AND REACH THOUSANDS OF
QUALIFIED SCIENTISTS EACH MONTH.

PHYSICS TODAY | JOBS
WWW.PHYSICSTODAY.ORG/JOBS

Threshold voltage shift and formation of charge traps induced by light irradiation during the fabrication of organic light-emitting diodes

Yutaka Noguchi,^{1,2,a)} Naoki Sato,² Yuya Tanaka,² Yasuo Nakayama,¹ and Hisao Ishii^{1,2}

¹Center for Frontier Science, Chiba University, 1-33 Yayoi-cho, Inage-ku, Chiba 263-8522, Japan

²Graduate School of Advanced Integration Science, Chiba University, 1-33 Yayoi-cho, Inage-ku, Chiba 263-8522, Japan

(Received 21 March 2008; accepted 30 April 2008; published online 23 May 2008)

We examined the effects of ambient light on the device properties of an organic light-emitting diode, indium tin oxide/4,4'-bis[*N*-(1-naphthyl)-*N*-phenylamino]-biphenyl (α -NPD)/tris-(8-hydroxyquinolate) aluminum (Alq₃)/Al, during fabrication using displacement current measurement. Light irradiation induces a shift in the threshold voltage for hole injection and results in the formation of charge traps in the Alq₃ layer. The voltage shift implies a reduction in charge density at the α -NPD/Alq₃ interface. The origin of the interfacial charge can be attributed to dipole moment ordering in the Alq₃ layer. © 2008 American Institute of Physics.

[DOI: 10.1063/1.2936084]

The device properties of an organic light-emitting diode (OLED) comprising 4,4'-bis[*N*-(1-naphthyl)-*N*-phenylamino]-biphenyl (α -NPD) or its derivatives and tris-(8-hydroxyquinolate) aluminum (Alq₃) have been investigated by various methods including displacement current measurement (DCM).¹⁻⁴ Brütting *et al.* revealed that hole injection from the anode to the α -NPD layer mostly occurs at biases lower than the built-in voltage (V_{bi}), and clarified the hole injection properties with negative charges of about -1.1 mC/m^2 at the α -NPD/Alq₃ interface.⁴ Interfacial charge is intrinsic to the α -NPD/Alq₃ interface and is important for not only device operation,⁴ but also device degradation.⁵ The microscopic origin of this charge, however, remains to be clarified.

Studies have suggested the presence of a giant surface potential (GSP) across the Alq₃ film to be a possible source. For example, Ito *et al.* reported the buildup of a GSP, during the formation of an Alq₃ film on a metal substrate under dark conditions, caused by dipole moment ordering in the Alq₃ film.⁶ The GSP grows linearly as a function of film thickness (reaching 28 V at a film thickness of 560 nm) and induces a surface charge on the film with a constant density of approximately 1.32 mC/m^2 .⁷ This value is similar to the charge density at the α -NPD/Alq₃ interface. If orientation polarization of the Alq₃ film persists in the OLEDs, the surface charge of the Alq₃ layer should act as the charge at the α -NPD/Alq₃ interface.

Interestingly, the GSP disappears on light irradiation during or after film deposition if the photon energy exceeds the absorption edge of Alq₃. Two mechanisms have been proposed to remove a GSP: (i) Photoinduced formation of compensation charges and (ii) dipole moment disordering in the Alq₃ film.^{6,8-10} Several research groups have investigated the mechanisms leading to a GSP, but little is still known about how the GSP and its decay affect the properties of OLEDs comprising Alq₃ films.

In this letter, we report the effects of ambient light on the device properties of an OLED, indium tin oxide (ITO)/ α -NPD/Alq₃/Al, during fabrication. Light irradiation leads to the formation of charge traps and a higher threshold

voltage for hole injection. The voltage shift corresponds to a decrease in the charge at the α -NPD/Alq₃ interface. Considering the similarities between interfacial charge and GSP, the origin of the charge can be attributed to dipole moment ordering in the Alq₃ film.

The structure of the device being studied is ITO/ α -NPD (40 nm)/Alq₃ (60 nm)/Al (100 nm), with a device active area of approximately 1.77 mm^2 [Fig. 1(a)]. The organic layers and Al electrode were successively fabricated on an ITO-coated glass substrate using a conventional vacuum sublimation technique. Two types of devices (denoted as devices A and B) were fabricated under the same conditions, except for the presence of ambient light during deposition. Throughout the deposition process, device A was fabricated under dark conditions while device B was irradiated by room light through a glass bell jar ($\sim 1.0 \mu\text{W/cm}^2$). The devices were then transferred to a vacuum probe station. DCM and current density-voltage-luminance (J - V - L) measurements were performed in the dark at room temperature.

DCM involves capacitance-voltage measurement and was specifically introduced to analyze organic diodes.^{11,12} Egusa *et al.* conducted extensive studies to investigate the properties of model OLED interfaces.¹ DCM enables us to characterize the behavior of carriers and trapped charges and that of dielectrics in organic electronic devices.^{5,13,14} The principle of DCM is simple: A triangular wave bias is applied to the device and the current response is measured. The experimental setup for DCM is shown in Fig. 1(a). We employed the FCE-1 measurement system for ferroelectrics

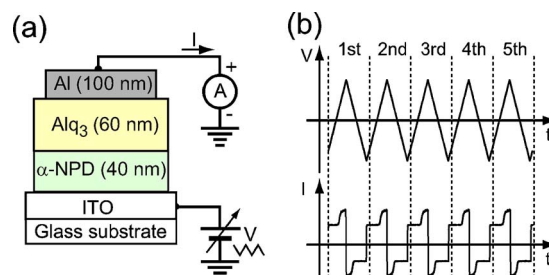


FIG. 1. (Color online) (a) Schematic illustration of sample structure and experimental setup. (b) Schematic illustration of applied triangular wave and current response.

^{a)}Electronic mail: y-noguchi@faculty.chiba-u.jp.

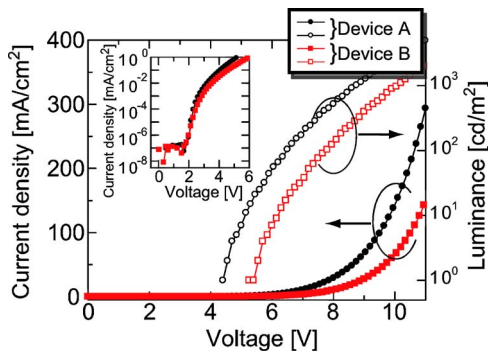


FIG. 2. (Color online) Typical J - V - L curves of devices A and B. The inset shows the semilog plots of J - V curves around the threshold voltages.

(Toyo Corp.). The DCM curves were measured by applying biases within ± 5.0 V to the ITO layer, with reference to the Al electrode, at a sweep rate of 1 V/s. The DCM curves were measured over five sequential cycles of the triangular bias sweep [Fig. 1(b)]. The J - V - L curves were measured using a source-measure unit (model 237, Keithley) and a luminance meter (Bm-9, Topcon).

Figure 2 shows the typical J - V - L curves of devices A and B. The conductivity and luminance of device B are lower than those of device A. This difference may be due to

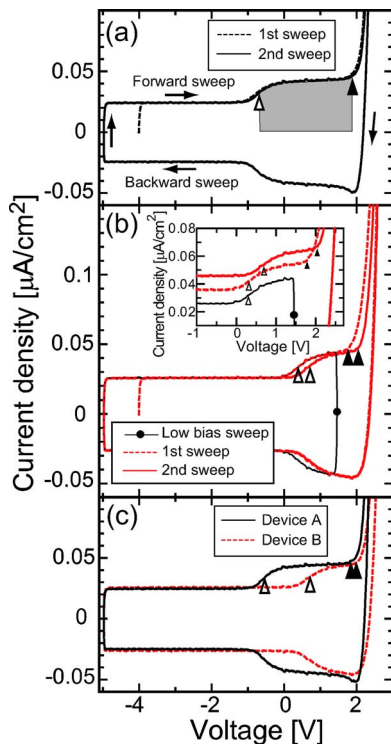


FIG. 3. (Color online) Typical DCM curves of devices A and B (sweep rate: 1 V/s). The open and closed triangles show the voltage of hole injection from the ITO layer to the α -NPD layer (V_{inj}) and from the α -NPD layer to the Alq_3 layer (V_{th}), respectively. (a) The DCM curves obtained by applying the first (broken line) and second (solid line) bias sweeps are shown. The arrows indicate the direction of the bias sweep and the halftone area corresponds to the number of holes accumulated at the α -NPD/ Alq_3 interface. (b) Typical DCM curves of device B as a function of the applied triangular wave bias. The solid line marked by the closed circle is the DCM curve of the lower bias sweep obtained before applying biases higher than V_{th} . The broken and solid lines (without marks) are the DCM curves obtained by applying the first and second bias sweeps, respectively. The inset shows DCM curves around the biases of V_{inj} and V_{th} in the forward sweep. Each curve is plotted for clarification. (c) The DCM curves of device A (solid line) and device B (dashed line) in the steady state.

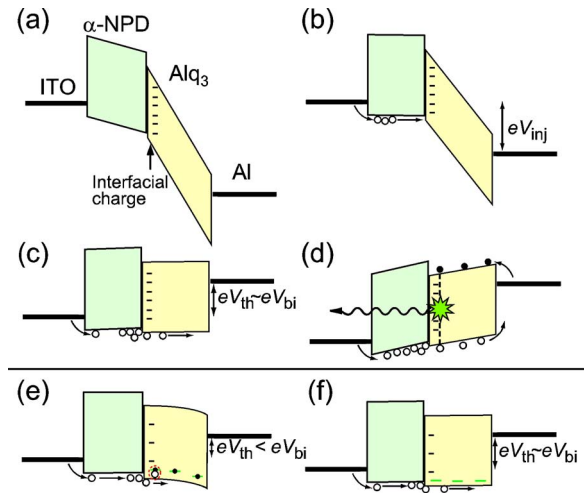


FIG. 4. (Color online) [(a)–(d)] Schematic energy diagrams of device A at (a) the start voltage, (b) V_{inj} , (c) V_{th} , and (d) the voltage at light emission. [(e)–(f)] Schematic energy diagram of device B at V_{th} for the (e) first and (f) second sweeps. The V_{th} of the first sweep is lower than V_{bi} due to the negative trapped charges in the Alq_3 layer. For the second sweep, V_{th} is close to V_{bi} , because some of the injected holes are trapped in the Alq_3 layer during the first sweep, which compensates for the negative trapped charges.

a combination of factors related to, for example, the properties of the interfaces, carriers, and charge traps. Although it is difficult to pinpoint the exact reason from the J - V - L curves, the DCM results at the biases below arising the actual current provide us useful information on the origin as described later.

We first explain the DCM curve of device A before discussing the effects of ambient light. Figure 3(a) shows the typical DCM curves of device A. The triangular bias sweep starts at -4 V. Around the start voltage, the current intensity is at the base line ($0.024 \mu A/cm^2$), indicating that no carrier exists in the device [Fig. 4(a)]. Subsequently, the current rises at a voltage of -0.71 V (V_{inj}) due to the hole injection from the ITO to the α -NPD layer [Fig. 4(b)]. We defined V_{inj} as the inflection point of the step structure in the DCM curve. The current, again, keeps a constant intensity ($0.043 \mu A/cm^2$) until the biasing voltage reaches 1.90 V (V_{th}), because of hole accumulation at the α -NPD/ Alq_3 interface. V_{th} corresponds to the threshold voltage of the actual current (see inset of Fig. 2) and it agrees well with V_{bi} (1.9 V) of the device, estimated from the open-circuit voltage during white light irradiation. Therefore, the holes accumulated at the α -NPD/ Alq_3 interface can then proceed to the Alq_3 layer and flow out to the Al electrode [Fig. 4(c)].¹⁵ From the observed V_{inj} and V_{th} , the interfacial charge density σ_0 is estimated as⁴

$$\sigma_0 = -C_{Alq}(V_{th} - V_{inj})/S, \quad (1)$$

where C_{Alq} is the capacitance of the Alq_3 layer, and S is the device active area. The equation indicates that the injected holes are captured at the α -NPD/ Alq_3 interface to compensate for the interfacial charge. At V_{th} , the amount of injected holes becomes equal to that of the interfacial charge. Finally, the electrons are injected from the Al electrode to the Alq_3 layer and light is emitted [Fig. 4(d)]. The DCM curve is almost symmetrical to the $I=0$ axis of applied biases lower than V_{th} . Therefore, in the backward sweep, the reverse of processes described in Figs. 4(a)–4(d) is expected.

Figure 3(b) shows the typical DCM curves of device B as a function of applied triangular bias with the number of sweep cycles. The DCM curve of the second sweep, of device B shifted slightly from that of the first sweep, if a bias higher than V_{th} was applied. We confirmed that the DCM curves traced the same path as that of the second sweep while applying further bias sweeps, and conclude that the device was in a steady state after the sweeps.

The effect of ambient light during device fabrication is evident from the DCM curves. In the steady state, V_{inj} estimated from the DCM curve of device B is significantly larger than that of device A, although the V_{th} values are similar [Fig. 3(c) and inset of Fig. 2]. These results are attributed to the difference in σ_0 ($\propto V_{th} - V_{inj}$) of devices A and B. Using Eq. (1), the σ_0 of device A is obtained from the DCM curves as -1.13 ± 0.03 mC/m² (10 samples), while that of devices B is -0.56 ± 0.13 mC/m² (13 samples). The σ_0 of device A is very stable and in good agreement with that reported previously.^{4,5} Here it should be noted that ambient light was controlled only during the film deposition process. After device fabrication, both devices were incidentally or intentionally exposed to light; however, further changes in σ_0 were not observed. From these results, we conclude that σ_0 is reduced by light irradiation during device fabrication.

We now report similarities between the charge at the α -NPD/Alq₃ interface and the GSP of the Alq₃ film. As described earlier, the surface charge density induced by the GSP is approximately 1.32 mC/m² and is independent of film thickness. Similar values have been reported for different substrates by other groups, e.g., 1.25 mC/m² for Au substrate⁸ and 0.80–1.33 mC/m² for Al substrates.¹⁰ The observed σ_0 of device A is comparable to these values and independent of Alq₃ film thickness.^{4,15} In addition, both σ_0 and the GSP are reduced by light irradiation during film deposition. These results suggest that the charge at the α -NPD/Alq₃ interface and the GSP could have the same origin, i.e., dipole moment ordering in the Alq₃ film.

In our devices, σ_0 did not change even if the devices were exposed to white light (LEDs or halogen lamp, ~ 10 mW/cm²) after fabrication. In contrast, the GSP decay results from light irradiation even after film deposition.^{6,8,9} The difference in the decay mechanism between the GSP and interfacial charge could be a reason for this. The GSP was examined on the free surface of the Alq₃ film deposited on a metal or glass substrate without applying an external biasing voltage. Thus, when carriers are formed in the film by light irradiation, they are captured at the film surface because of surface charges. Consequently, the GSP disappears even if dipole moment ordering persists in the film. In the device, however, σ_0 is unlikely to be reduced by the compensation charges, because the charges can be removed (except in the strongly trapped case) by applying an external biasing voltage. Thus, the interfacial charges in the device remain as long as the dipole moment in the film is ordered.

In Fig. 3(b), the DCM curve obtained by applying a bias lower than V_{th} is shown, indicating a steady state before hole injection into the Alq₃ layer. This curve and that obtained by the first forward sweep for a higher bias ($\geq V_{th}$) coincide with each other [inset of Fig. 3(b)], indicating a slight shift of V_{inj} and V_{th} caused by hole injection into the Alq₃ layer. This shift suggests that part of the holes injected into the Alq₃ layer were trapped during the first forward sweep [Fig. 4(e)], holes caused variations in the electric field

distribution [Fig. 4(f)]. Because V_{inj} and V_{th} shift almost equally and V_{th} of the first sweep is less than V_{bi} (1.9 V), there should be an attracting electric field to trap the holes in the Alq₃ layer [Fig. 4(e)]. On the other hand, device A was mostly trap-free. It seems that negative trapped charges, formed due to light irradiation during device fabrication, contributed to such an electric field in the device.

Kondakov *et al.* reported that σ_0 decreased with device degradation and device efficiency.⁵ Our findings show that light irradiation during device fabrication caused a similar effect even in fresh devices and implies that decreasing the orientation polarization in the Alq₃ layer may be responsible for device degradation. This scenario is consistent with observations of relatively lower conductivity and luminance in device B (Fig. 2).

In summary, we found that light irradiation during device fabrication reduces the charge density at the α -NPD/Alq₃ interface. The relationship between interfacial charge density and the GSP of an Alq₃ film was discussed. The results suggest that the charge at the α -NPD/Alq₃ interface is due to dipole moment ordering in the Alq₃ film. We also found that light irradiation causes charge traps in the Alq₃ layer. It should be noted that most OLED materials have a permanent dipole moment because the lower symmetry in molecular structure is designed to suppress crystallization and form amorphous films. A similar effect may occur in devices composed of materials possessing a permanent dipole moment. Also, ambient light should be considered for device fabrication.

We would like to thank Professor Wolfgang Brütting and Mr. Yoshinori Fukuda for fruitful discussions. This work was financially supported by the 21st COE Project of Chiba University (Frontiers of Super Functionality Organic Devices), Grants-in-Aid for Scientific Research (Nos. 19655065, 18350093, 14GS0213, and 17710110), and Core To Core Program of Japan Society for the Promotion of Science “Electronic Structure and Electronic Processes in Films and Interfaces Related to Organic Electronics.”

¹S. Egusa, A. Miura, N. Gemma, and M. Azuma, *Jpn. J. Appl. Phys., Part 1* **33**, 2741 (1994).

²M. Matsumura, Y. Jinde, T. Akai, and T. Kimura, *Jpn. J. Appl. Phys., Part 1* **35**, 5735 (1996).

³F. Röhlfing, T. Yamada, and T. Tsutsui, *J. Appl. Phys.* **86**, 4978 (1999).

⁴W. Brütting, S. Berleb, and A. G. Mückl, *Org. Electron.* **2**, 1 (2001).

⁵D. Y. Kondakov, J. R. Sandifer, C. W. Tang, and R. H. Young, *J. Appl. Phys.* **93**, 1108 (2003).

⁶E. Ito, N. Hayashi, H. Ishii, N. Matsuie, K. Tsuboi, Y. Ouchi, Y. Harima, K. Yamashita, and K. Seki, *J. Appl. Phys.* **92**, 7306 (2002).

⁷In Ref. 6, surface charge density was determined to be 0.44 mC/m². It was derived by subtracting electronic polarization from orientation polarization. The latter is necessary for our discussion. Throughout this letter, we assumed the dielectric constant of Alq₃ to be 3.0.

⁸K. Sugi, H. Ishii, Y. Kimura, M. Niwano, E. Ito, Y. Washizu, N. Hayashi, Y. Ouchi, and K. Seki, *Thin Solid Films* **464-465**, 412 (2004).

⁹K. Yoshizaki, T. Manaka, and M. Iwamoto, *J. Appl. Phys.* **97**, 023703 (2005).

¹⁰N. Kajimoto, T. Manaka, and M. Iwamoto, *Jpn. J. Appl. Phys., Part 1* **46**, 2740 (2007).

¹¹A. J. Twarowski and A. C. Albrecht, *J. Chem. Phys.* **70**, 2255 (1979).

¹²K. Iriyama, M. Shiraki, K. Thuda, A. Okada, M. Sugi, S. Iizima, K. Kudo, S. Shiokawa, T. Moriizumi, and T. Yasuda, *Jpn. J. Appl. Phys.* **19**, Suppl. 19-2, 173 (1980).

¹³S. Ogawa, Y. Kimura, H. Ishii, and M. Niwano, *Jpn. J. Appl. Phys., Part 2* **42**, L1275 (2003).

¹⁴S. Ogawa, Y. Kimura, M. Niwano, and H. Ishii, *Appl. Phys. Lett.* **90**, 033504 (2007).

¹⁵N. Sato, Y. Noguchi, Y. Tanaka, Y. Nakayama, and H. Ishii (unpublished).